Synthesis, Characterization, and Physical Properties of New Ferroelectric Liquid Crystalline Materials: Block Copolymers

A. Omenat,† R. A. M. Hikmet, J. Lub,* and P. van der Sluis

Philips Research Laboratories, Prof. Holstlaan 4, 5656 AA Eindhoven, The Netherlands

Received February 6, 1996; Revised Manuscript Received July 12, 1996[⊗]

ABSTRACT: As part of our research on new ferroelectric liquid crystalline materials, we present the synthesis, characterization, and physical properties of a new family of polymeric materials, namely AB block copolymers consisting of a non-liquid crystalline chain [poly(isobutyl vinyl ether)] and a chiral liquid crystalline block. The combination of both features gives rise to the appearance of interesting effects on the properties of the polymers: they show the ferroelectric chiral smectic C mesophase at room temperature with low viscosities and low birefringence, due to the presence of the non-liquid crystalline chain. The chiral smectic C phase exhibits the characteristic switching under electric fields. Its electro-optical behavior has been characterized and is different than that of the parent homopolymer. The block copolymers show the typical microphase separation of the two blocks which has been observed by small angle X-ray scattering.

Introduction

Since the discovery of fast electro-optic switching in surface-stabilized ferroelectric liquid crystal (SSFLC) cells,[1] ferroelectric liquid crystals have attracted great interest for display applications. Currently, SSFLC have the advantage of high speed, bistability, and a wide viewing angle over conventional nematics, but they present other problems, such as the difficulty of obtaining good uniform orientation and sustaining it, the necessity of small cell gaps, production of gray levels, and the low shock resistance of the cells. In the last few years new research efforts have been made in order to find solutions to these problems, which have resulted in the development of new ferroelectric systems: oligomeric and polymeric liquid crystalline materials,[2−11] polymer dispersed ferroelectric systems,[12] and anisotropic ferroelectric gels.[13]

Polymeric ferroelectric liquid crystals (FLC) show some advantages with respect to low molecular weight FLC, since they are easy to process, show good shock resistance, and open the possibility for making flexible displays. On the other hand, the main disadvantages of liquid crystalline polymers are their high viscosity and, thus, slow response time to an applied electric field and the poor reproducibility of the polymerization methods used to obtain these materials.

The option of using oligomeric liquid crystals appeared to be a logical solution to these problems, and in this direction, several systems have been described recently.[14−17] This type of material shows good ferroelectric properties at room and higher temperatures.

Another approach to achieve fast switching ferroelectric polymers exhibiting the chiral smectic phase at low temperature consists of the use of copolymers:[18−22] the presence of a non-liquid crystalline chain in the polymer would reduce its viscosity. Most of the copolymers described are random copolymers. Chiellini et al.[23] have reported the synthesis and electroclinical properties of chiral smectic A block copolymers obtained from macroinitiators. In this publication, we present a new ferroelectric liquid crystalline system based on block copolymers consisting of a liquid crystalline chain and an amorphous block [poly(isobutyl vinyl ether)] (See Chart 1). By using a sequential living polymerization method it is possible to synthesize block copolymers with controlled molecular weight, controlled relative compositions of the different blocks, and narrow molecular weight distribution. We have, thus, the ability to synthesize tailor-made polymeric materials with total reproducibility by adjusting the concentration of monomer vs initiator.

These materials, which are composed of incompatible block segments, give rise to a microdomain morphology, making it possible to combine the properties of two completely different polymers without macroscopic phase separation.[24−28] The presence of the non-liquid crystalline segment in the polymers provides interesting changes in the properties of the ferroelectric material, such as birefringence, which can be controlled easily by adjusting the relative composition of the blocks in the copolymer.

The materials show a chiral smectic C phase at room temperature and good alignment by shearing between two glass plates without using any orientation layer. The electro-optical behavior of the chiral mesophase of the block copolymers is different from that of the corresponding liquid crystalline homopolymer.

In this study, we describe the synthesis and characterization of these new types of materials, as well as their ferroelectric properties and the effect of the block copolymer composition on their behavior.

Experimental Section

Materials. 1,10-Phenanthroline (99+%), palladium(II) acetate, *p*-toluenesulfonyl chloride (99+%), and *n*-butyl vinyl ether (98%), all from Acros Chimica, and (*S*)-(−)-ethyl lactate (98%) and 4′-hydroxy-4-biphenylcarboxylic acid (99%), both from Aldrich, were used as received. 11-Bromo-1-undecanol (98%) (Aldrich) was distilled under reduced pressure prior to use. All the solvents were obtained from Merck and dried according to conventional methods. (1,10-Phenanthroline)-palladium(II) diacetate was prepared according to a literature procedure.[29,30]

Isobutyl vinyl ether (IBVE) (99%) (Aldrich) was refluxed over calcium hydride and distilled twice under argon. Tin(IV) bromide (1.0 M solution in methylene chloride) (Aldrich) was used as received. The initiator **5** was prepared by electrophilic addition of hydrogen chloride to isobutyl vinyl ether in *n*-hexane.[31] Methylene chloride (polymerization solvent) and *n*-hexane (solvent for **5**) were distilled twice over

†Current address: Dpto. Química Orgánica-Química Física, Instituto de Ciencia de Materiales de Aragón, Universidad de Zaragoza, 50009 Zaragoza, Spain.

⊗ Abstract published in *Advance ACS Abstracts,* September 15, 1996.

S0024-9297(96)00185-4 CCC: $12.00

Chart 1. Structure of the Block Copolymers

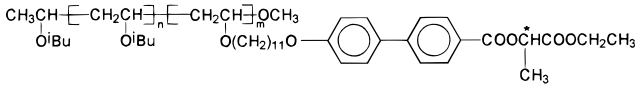

calcium hydride under argon into a flask containing 3Å molecular sieves.

Techniques. ^{1}H-NMR spectra were recorded on a Bruker DPX 300 spectrometer. Tetramethylsilane was used as an internal standard and deuterated chloroform as solvent.

A Perkin-Elmer DSC-7 differential scanning calorimeter was used to determine the temperatures and enthalpies of transition of the polymers. In all cases, the heating and cooling rates were 10 °C/min.

A Reichert optical microscope provided with a Mettler FP52 hot stage was used to observe the thermal transitions and to analyze the textures of the mesophases.

The molecular weights and polydispersities of the polymers were determined by gel permeation chromatography (GPC).

All the samples were dissolved in chloroform (Merck p.a.) in a concentration of 1 mg/mL. Of each sample, 25 μL was injected on two columns (PL-gel-5 μL-mixed C, with guard column μL-gel 5 μL-GUARD; linear for Mw= 200−3 000 000), and was eluted with chloroform (Acros, LC-quality). The flow was 1 mL/min and the UV detector was fixed at 254 nm. The column was calibrated with polystyrene standards (Easy-cal).

The X-ray measurements were carried out on a home-built system consisting of a sealed X-ray tube (Cu Kα radiation), a primary graphite monochromator, a pinhole collimator, a sample stage, and a Siemens Hi-Star area detector. All components were mounted on an optical bench to provide maximal flexibility and easy alignment. For the experiments at elevated temperatures, the sample was mounted in a Mettler FP52 hot stage. Wide angle X-ray (WAXS) patterns were recorded with a sample-to-detector distance of 9 cm and small angle X-ray (SAXS) patterns were recorded with a sample-to-detector distance of 49 cm. The pinholes of the collimator were 0.25 mm in diameter and 15 cm apart. Background and air scattering were measured separately and substracted to give the final diffraction patterns.

The samples were films made at room temperature (22 °C) by shearing the polymers on a glass surface with the aid of a metallic bar.

The refractive indices of the polymers were measured using a thermostated Abbe refractometer.

The electro-optical behavior of the polymers was studied using a polarizing optical microscope provided with a photomultiplier. A wave generator was used to apply electric fields across the samples, and the electro-optical signals were displayed on a digital oscilloscope. The data obtained were transferred to a computer where they were further processed.

Synthesis of monomer 4. The reaction sequence is shown in Scheme 1.

Synthesis of 11-Bromoundecanyl Vinyl Ether (1). A mixture of 17.58 g (0.07 mol) of 11-bromo-1-undecanol, 175 mL of *n*-butyl vinyl ether, and 950 mg (2.33 mmol) of (1,10-phenanthroline)palladium(II) diacetate in 40 mL of dry chloroform was stirred at 60 °C under argon for 3 h. The reaction mixture was filtered through a pad of Celite and the solution obtained was concentrated under reduced pressure to yield a yellow oil, which was purified by column chromatography (silica gel, CH_2Cl_2 as an eluent). The product obtained is a colorless liquid. Yield: 17 g, 88%. ^{1}H-NMR ($CDCl_3$) (δ, ppm): 6.48 (dd, 1H), 4.18 (dd, 1H), 3.98 (dd, 1H), 3.68 (t, 2H), 3.40 (t, 2H), 1.87 (m, 2H), 1.66 (m, 2H), 1.50−1.22 (m, 14H).

Synthesis of Ethyl *O*-(*p*-Toluensulfonyl)lactate (2). *p*-Toluenesulfonyl chloride (57.15 g, 0.3 mol) was dissolved in 50 mL of dry pyridine under argon. The solution was cooled down to −7 °C, and 29.5 g (0.25 mol) of (*S*)-(−)-ethyl lactate was added dropwise with stirring. The temperature of the reaction must not be higher than 5 °C. After the complete addition of ethyl lactate, the reaction mixture was stirred at 0 °C for 2 h.

Water−ice (50 mL) was added to the reaction mixture followed by 30 mL of hydrochloric acid (37%) and 60 mL of water−ice. The mixture was extracted with diethyl ether (2 × 100 mL), and the organic layer was washed with a saturated solution of sodium chloride, dried over magnesium sulfate, filtered, and concentrated by rotary evaporation, to yield **2**, as white crystals (50 g, 75%). ^{1}H-NMR ($CDCl_3$) (δ, ppm): 7.80 (d, 2H), 7.33 (d, 2H), 4.91 (q, 1H), 4.10 (q, 2H), 2.45 (s, 3H), 1.50 (d, 3H), 1.20 (t, 3H).

Synthesis of 3. A mixture of 15 g (0.07 mol) of 4′-hydroxy-4-biphenylcarboxylic acid and 6 g (0.07 mol) of sodium bicarbonate in 60 mL of *N*,*N*-dimethylacetamide (DMAC) was stirred at 90 °C until the evolution of CO_2 had ceased. To this solution was added 19.04 g (0.07 mol) of **2**. The reaction mixture was stirred at 90 °C for 2 h, cooled to room temperature, and poured into water. The white precipitate is filtered off and recrystallized from ethanol−water (1/1). Compound **3** is obtained as white crystals (17.7 g, 81%). ^{1}H-NMR ($CDCl_3$) (δ, ppm): 8.12 (d, 2H), 7.62 (d, 2H), 7.50 (d, 2H), 6.98 (d, 2H), 5.56 (s, 1H), 5.33 (c, 2H), 4.28 (c, 2H), 1.65 (d, 3H), 1.28 (t, 3H). Mp: 156 °C.

Synthesis of Monomer 4. Compound **3** (7.5 g, 0.024 mol), 8.25 g (0.06 mol) of potassium carbonate, and 6.92 g (0.025 mol) of **1** were dissolved in 60 mL of butanone. The reaction mixture was refluxed for 24 h and then filtered to remove the salts formed during the reaction. The filtered solution was concentrated under reduced pressure, and the brown oil obtained was purified by column chromatography (silica gel, CH_2Cl_2 as eluent), to give compound **4**, which is further purified by recrystallization from ethanol−water (3/1). Yield: 8 g, 65%. ^{1}H-NMR ($CDCl_3$) (δ, ppm): 8.10 (d, 2H), 7.62 (d, 2H), 7.57 (d, 2H), 7.00 (d, 2H), 6.48 (dd, 1H), 5.35 (c, 1H), 4.27 (c, 2H), 4.18 (dd, 1H), 4.03 (t, 2H), 4.00 (dd, 1H), 3.70 (t, 2H), 1.85 (q, 2H), 1.70 (q, 2H), 1.66 (d, 3H), 1.55−1.20 (m, 14H), 1.18 (t, 3H).

Thermal properties (DSC): mp 31.2 °C. Monotropic smectic A mesophase appears at 29.4 °C on cooling of the isotropic liquid.

Polymerization. The homopolymerization and the sequential polymerization of the vinyl ether monomers were carried out according to the method described by Ohmura et al.[32] (See Scheme 2).

Procedure. Sequential living cationic polymerization of vinyl ethers was carried out under argon in a round-bottomed 50 mL flask equipped with a three-way stopcock and a magnetic stirring bar. All reagents were transferred via dried syringes.

A typical example of isobutyl vinyl ether (IBVE)-**4** block copolymerization is as follows: To a cooled IBVE solution (0.375 M, 8 mL) in CH_2Cl_2 at −78 °C was added a solution of initiator **5** (0.15 mmol) with vigorous stirring. After 15 min a solution of monomer **4** (0.2 mmol in 2 mL of CH_2Cl_2) was added. The polymerization was quenched after 1 h with ammoniacal methanol (3 mL). The solution was poured into methanol and the polymer precipitated. The polymer was purified by repeated precipitation into methanol. No monomers were detected by spectroscopic and chromatographic techniques (Yields: 70−80%).

Results and Discussion

Synthesis and Characterization of the Polymers. The cationic polymerization of vinyl ethers with the system IBVE−HCl/$SnBr_4$ gave excellent results in obtaining liquid crystalline block copolymers with narrow molecular weight distribution. The isolation and purification of the polymers are simple, giving high yields of the final materials, with the relative composition determined by the initial relative concentration of the monomers.

The investigated polymers (homopolymer and block copolymers) were characterized using ^{1}H-NMR, GPC, DSC, and polarizing optical microscopy. Their molecular weights, polydispersities, and thermal properties are gathered in Table 1.

All the polymers show the chiral smectic C phase at room temperature. From the DSC data the T_g and the transition from the smectic phase to the isotropic liquid

Scheme 1. Synthesis of the Monomer 4

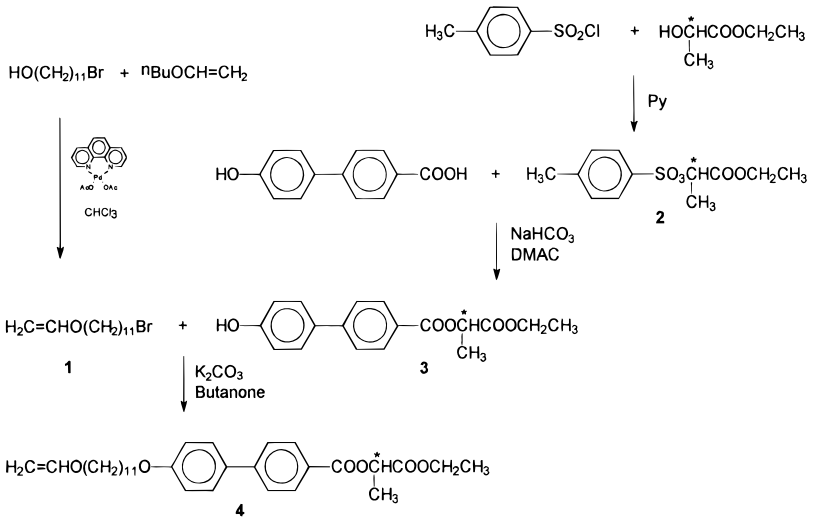

Scheme 2. Polymerization Method

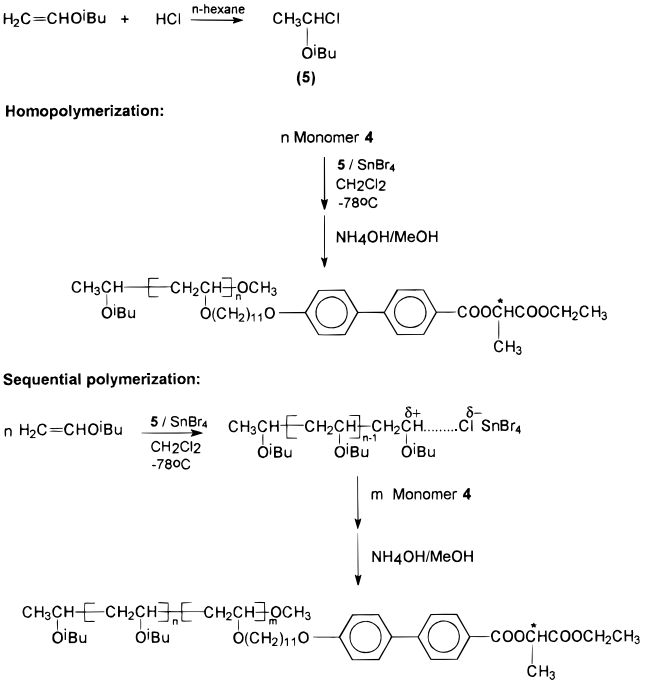

corresponding to the liquid crystalline block can be observed. For block copolymer **IV**, a DSC scan was performed down to −50 °C, which showed the glass transition corresponding to the poly(IBVE) block at −19 °C, which is direct proof of the inmiscibility of the blocks.

The differences in the transition temperatures arise from the difference in molecular weight of the polymers. If we compare the polymers with similar molecular weights (block copolymers **IV**, **V**, and **VI**), the temperature transitions are independent of the relative composition of the blocks in the copolymer. This fact is in agreement with a phase separation phenomenon taking place: the thermal behavior of the liquid crystalline chain is similar to that of the homopolymer and nearly affected by the nonmesogenic block. The values obtained for the transition enthalpy at the clearing point also indicate the phase-separated character of these polymers, as they do not differ much from the values expected taking into account the weight fraction of the liquid crystalline block in the copolymer (See Figure 1).

Finkelmann et al.[26] describe a similar behavior for nematic block copolymers, having poly(MMA) and polystyrene as non-liquid crystalline blocks. The values reported for ΔH_{N-I} in these cases are almost identical to those calculated from the ΔH_{N-I} of the corresponding mesogenic homopolymer. However, for smectic block copolymers, all of them having polystyrene as a non-liquid crystalline block, the values obtained for ΔH_{S-I} are 15−30% lower than those calculated.[24,27] In our case, values of ΔH_{S-I} 10−15% lower than calculated are obtained. This indicates that these block copolymers have a smaller disordered interphase between amorphous and smectic blocks than the other systems studied. The fact that the non-liquid crystalline block in our system is poly(IBVE), an aliphatic polymer, may have an influence on this behavior.

X-ray Measurements. WAXS and SAXS studies were carried out at room temperature on free-standing oriented films made from the polymers. A summary of the results obtained is presented in Table 2. WAXS measurements confirm the existence of the smectic C mesophase. An example is shown in Figure 2. The reflection corresponding to the lateral distance between mesogens is split into four peaks. From this splitting it is possible to calculate the tilt angle of the mesogens with respect to the normal to the smectic layers. In all the cases the tilt angle is around 30°.

The two different spacings observed at ∼17 and ∼31 Å can be explained as shown in Figure 3. The 31 Å spacing corresponds to the molecular length, whereas the distance of 17 Å is half of a bilayer spacing. Similar structures are described in refs 33 and 34. In the present case, the X-ray diffraction data indicate the same phenomenon taking place.

Besides these reflections indicating a smectic order in the liquid crystalline subphase, more intense reflections are observed in the small angle region (d ∼110 Å) corresponding to the phase separation of the blocks (Figure 2).

An interesting feature to be considered here is the relative orientation of the reflections corresponding to the smectic layers and to the blocks. It has been described for other liquid crystalline systems[24,27,28,35] based on block copolymers that in a lamellar morphology the smectic layers are oriented perpendicular to the block structure. This means that the main chain backbone of the mesogenic block tends to orient perpendicular to the interface of two microphases. On the other hand, when a cylindrical microstructure is present, the relative orientation of the smectic layers has been found to be parallel. This means that the

Table 1. Molecular Weight, Molecular Weight Distribution, and Thermal Properties of the Polymers

polymer	M_n[a]	D	Φ_{pIBVE}[b]	phase behavior[c]	ΔH_{S-I}[c] (J/g)
I	6500	1.40	–	g 9 °C, SmC* 45 °C, SmA 75 °C, I	6.5
II	23900	1.30	0.40	g 14 °C, SmC* 45 °C, SmA 82 °C, I	3.4
III	20500	1.27	0.34	g 16 °C, SmC* 44 °C, SmA 85 °C, I	4.3
IV	9600	1.26	0.33	g 11 °C, SmC* 44 °C, SmA 67 °C, I	4.0
V	8100	1.25	0.45	g 7 °C, SmC* 44 °C, SmA 68 °C, I	3.6
VI	8400	1.37	0.61	g 6 °C, SmC* 43 °C, SmA 65 °C, I	2.6

[a] Determined by GPC. [b] Volume fraction of poly(IBVE) in the block copolymer, *determined by ^1H NMR*, calculated using the densities 0.92 g/mL for poly(IBVE) and 1.11 g/mL for poly(**4**). [c] DSC data corresponding to the second heating scan. The transition SmC*–SmA is observed only by optical means. (g, glass transition; SmC*, chiral smectic C phase; SmA, smectic A phase; and I, isotropic liquid).

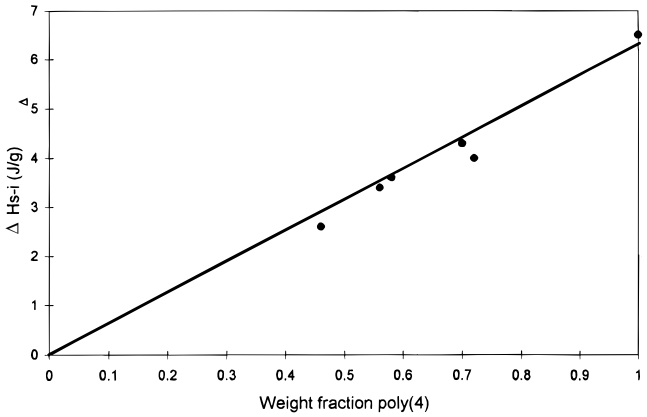

Figure 1. Enthalpy of the transition smectic to isotropic as a function of the weight fraction of the liquid crystalline block in the polymers.

Table 2. X-ray Diffraction Data of the Homopolymer and Block Copolymers at Room Temperature

	reflections (Å)					
	wide angle			small angle:	tilt angle	
polymer	d_0	d_1	d_2	d	(deg)	morphology
I	4.2	17.6	a	no reflection	32	
II	4.2	17.5	28.3	b		b
III	4.2	17.5	29.1	225, 138, 108	30	rods p(IBVE)
IV	4.2	17.1	31.8	107	29	lamellae
V	4.2	16.5	28.0	107	27	disks poly(**4**)[c]
VI	4.2	16.8	29.1	107	32	disks poly(**4**)[c]

[a] Unclear reflection. [b] Not determined. [c] Spheres or ellipsoids of poly(**4**) deformed by making the oriented film.

liquid crystalline chain tends to orient like a homopolymer, resulting in a parallel disposition of the main chain backbone with respect to the cylinders.[36]

In our case, the study of the patterns obtained for the polymer films in different directions (edge-on, perpendicular and parallel to the orientation direction of the film, and flat-on) provides some information about the morphology of the block copolymers. Figure 4 shows a representation of the different morphologies of the block copolymers deduced from the X-ray diffraction patterns.

For block copolymer **III** a morphology consisting of rods of poly(IBVE) in a matrix of the liquid crystalline poly(**4**) is found.

Block copolymer **IV**, with a volume fraction of poly(IBVE) similar to that of polymer **III**, shows a different diffraction pattern. In this case, the data obtained point to a lamellar structure in which the smectic layers are perpendicular to the blocks, as described above. The reason for this difference in the morphology of two block copolymers with approximately the same composition may be the different molecular weight and thus the different size of the resulting blocks. If we assume an extended conformation for the main chain of the liquid crystalline (LC) block of **IV** with an average of 15 repeating units of 2.5 Å length, its total length would

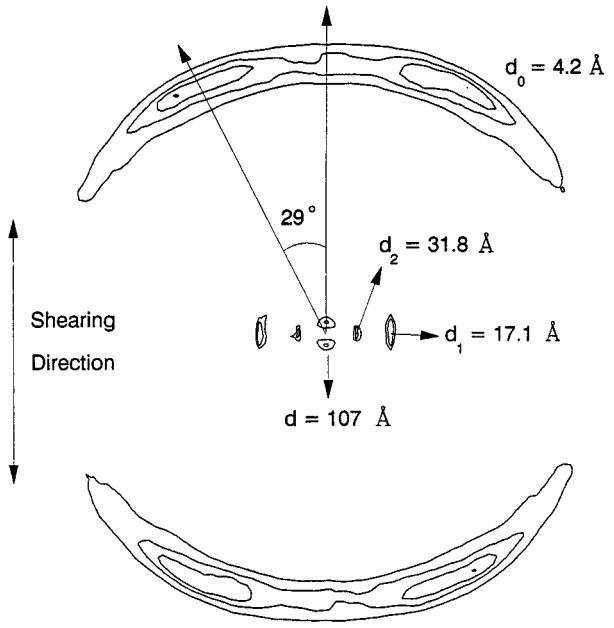

Figure 2. WAXS and SAXS pattern of block copolymer **IV**, edge-on parallel to the film shearing direction.

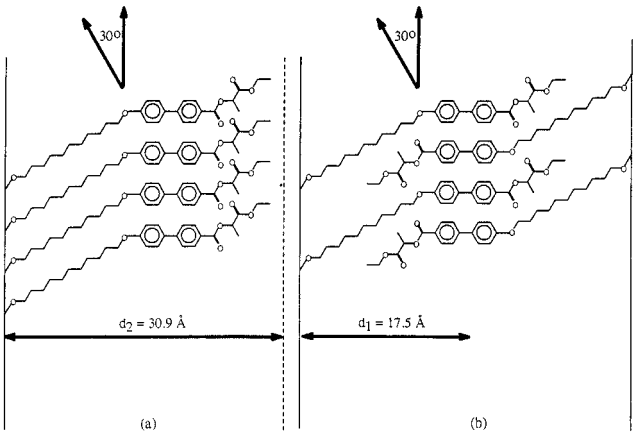

Figure 3. Proposed molecular arrangements in the smectic C phase for the polymers.

be 15 × 2.5 = 37.5 Å. As two of such segments will be included in the LC phase, then its thickness would be ~75 Å. The amorphous block which contains 33% of the volume of the polymer (see Table 1) would then have a thickness of ~25 Å. The X-ray measurement corresponds to the periodicity of the LC block spacing and the spacing of the amorphous block, which explains the frequently observed value of ~100 Å for the *d*-spacing.

For polymers **V** and **VI**, we find a parallel relative orientation of the smectic layers and the blocks. This fact indicates the absence of a lamellar microstructure. We assume that originally the morphology of these block copolymers consists of spheres of liquid crystals in a

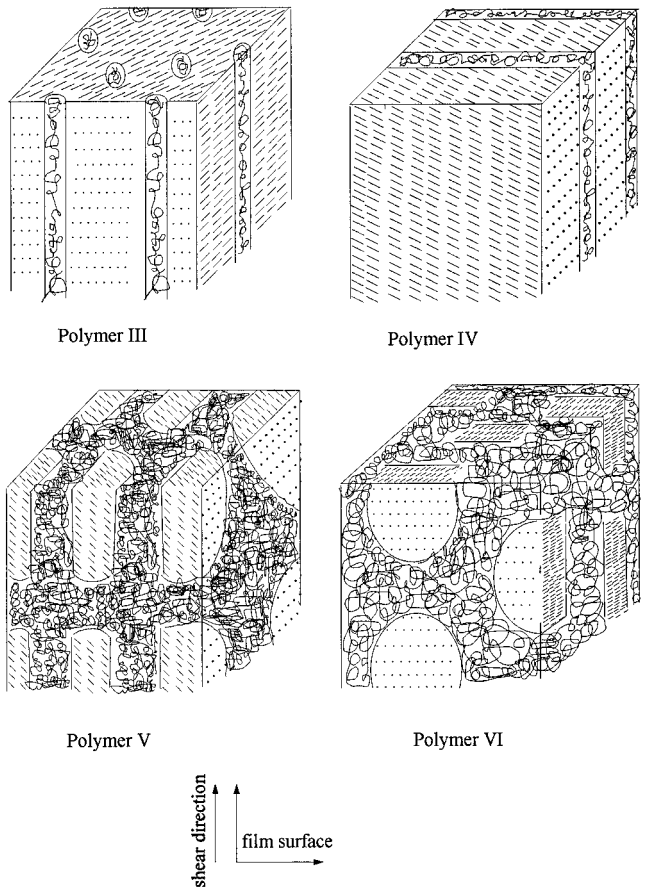

Figure 4. Morphologies of the block copolymers.

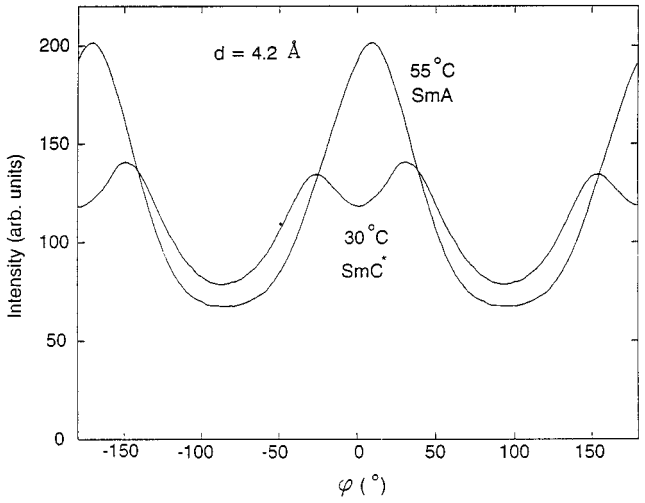

Figure 5. X-ray intensity as a function of rotation around the film normal at two temperatures for block copolymer **IV**.

matrix of poly(IBVE) as the polymeric chains contain no more than nine mesogenic units. In the process of making the oriented film, the material is pressed and sheared, which results in a deformation of the spheres. A morphology consisting of ellipsoids of the liquid crystalline block in a matrix of poly(IBVE) is expected, which is in accordance with the diffraction patterns obtained.

The representations of Figure 4 are in agreement with the molecular orientation observed by means of optical microscopy with polarized light. For polymers **III** and **VI** the films show a homeotropic orientation of the molecules (perpendicular to the film surface), while for polymers **IV** and **V** birefringent films are obtained, which indicates a planar orientation of the mesogenic units.

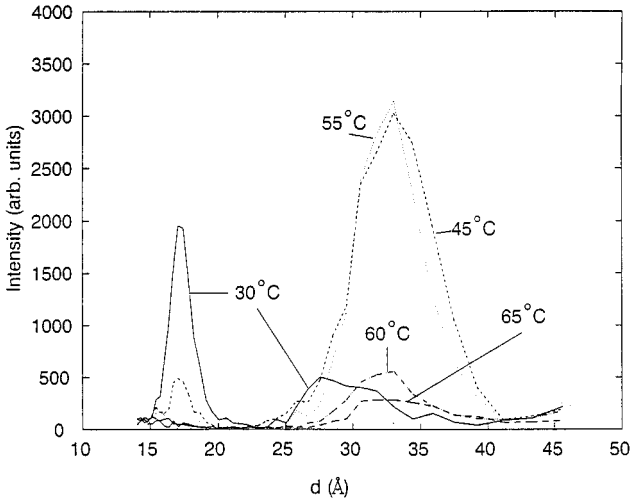

Figure 6. X-ray intensity in the smectic layer spacing region as a function of temperature for block copolymer **VI**.

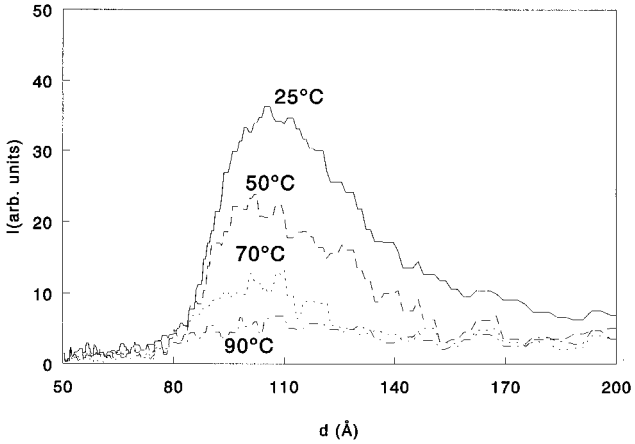

Figure 7. X-ray intensity in the small angle region as a function of temperature for block copolymer **IV**.

A WAXS study of copolymers **IV** and **VI** has been carried out at different temperatures. Figure 5 shows the variation of the intensity of the reflection at 4.2 Å as a function of rotation around the film normal at two temperatures for block copolymer **IV**. It gives a direct measure of the change of the tilt angle. As it can be seen at a temperature of 55 °C, the transition from the tilted smectic C phase to the orthogonal smectic A phase has taken place, since the four peaks observed for the smectic C* phase reduce to two peaks, corresponding to the smectic A phase.

Figure 6 shows the X-ray intensity of the smectic layers spacings as a function of temperature in the case of block copolymer **VI**. At 30 °C the two peaks corresponding to the parallel and antiparallel packings of the mesogens are present (see Table 2). At 45 °C these peaks are significantly reduced in intensity, while a new peak at ~33 Å appears. This value corresponds to the spacing of the layers of an orthogonal smectic phase. At 55 °C this trend continues. At higher temperatures the material becomes isotropic and the reflections disappear.

SAXS measurements of block copolymer **IV** were carried out at different temperatures. In this case, the sample was an unoriented film, giving rise to a ring in the small angle region. Figure 7 shows the results obtained for the integration of the reflection, represented as the intensity as a function of the distance *d*. The reflections due to the blocks are maintained even in the isotropic phase. Thus the phase separation is

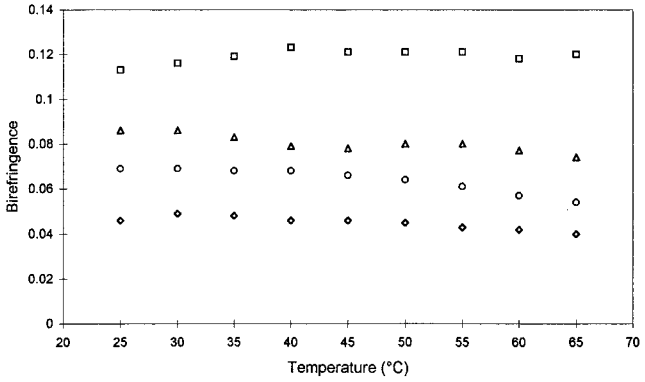

Figure 8. Birefrigence of the polymers as a function of temperature (□ = **I**, △ = **IV**, ○ = **V**, ◇ = **VI**).

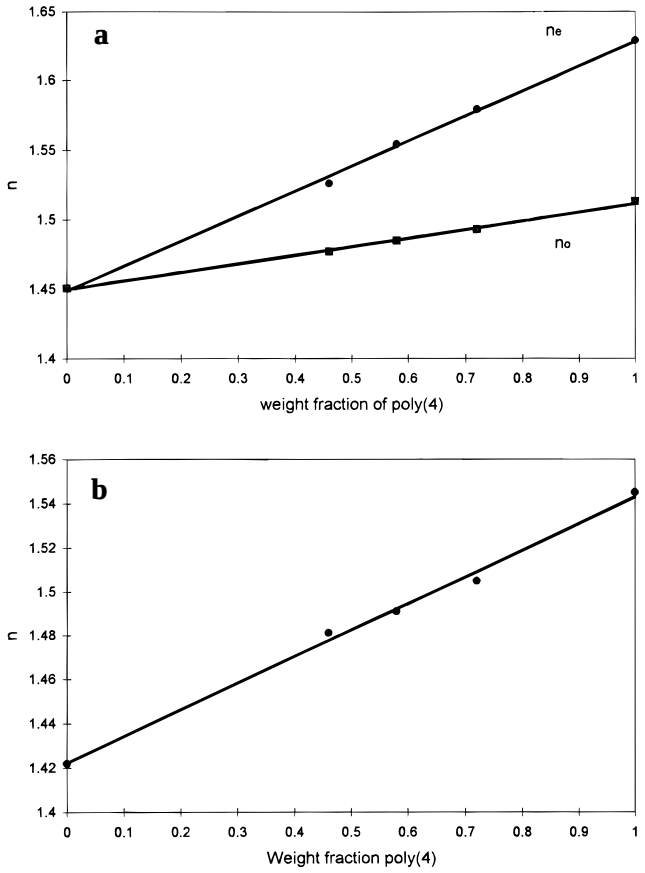

Figure 9. Refractive indices of the polymers as a function of the weight fraction of the liquid crystalline block. (a, 30 °C; b, 70 °C).

present to some extent at temperatures in which the block copolymer is isotropic.

Optical and Electro-Optical Studies. The refractive indices of the homopolymer **I** and block copolymers **IV**, **V**, and **VI** were measured as a function of temperature. Figure 8 shows the dependence of the birefringence of the polymers on temperature. It can be seen that the birefringence of the polymers decreases as the relative content of the non-liquid crystalline block increases. The variation of the refractive indices of the block copolymers as a function of the weight fraction of the liquid crystalline block is linear, as can be seen in Figure 9 for two different temperatures, in the smectic C mesophase (Figure 9a) and in the isotropic phase (Figure 9b). Thus, the birefringence of the polymeric material can be controlled easily by adjusting the relative composition of the two constituent blocks.

The electro-optical behavior of the polymers was studied by applying a triangular wave voltage and

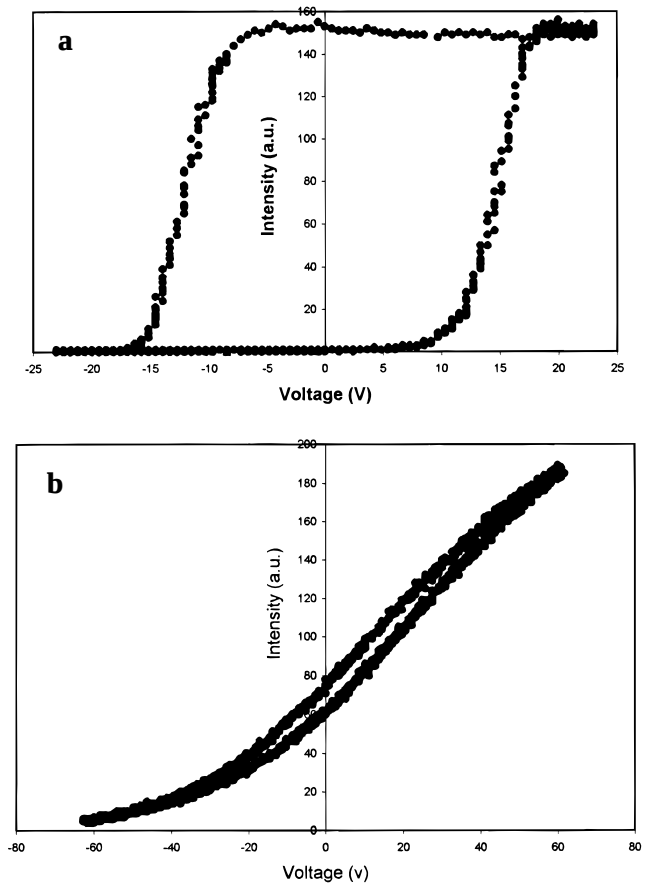

Figure 10. Electro-optical response of (a) homopolymer **I** at $T = 22$ °C and (b) block copolymer **V** at $T = 22$ °C obtained with a triangular wave voltage of 0.5 Hz.

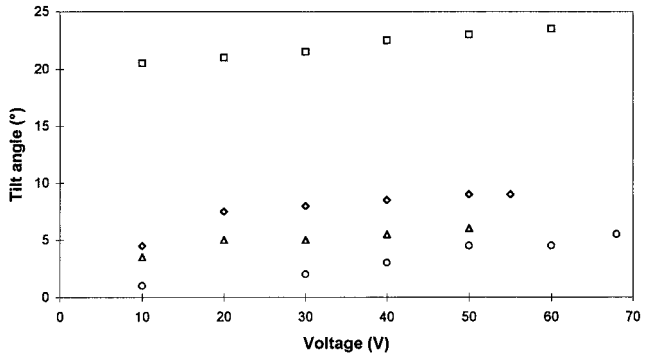

Figure 11. Tilt angle of homopolymer I and block copolymers **IV**, **V**, and **VI** as a function of applied voltage (□ = **I**, △ = **IV**, ○ = **V**, ◇ = **VI**).

measuring the light intensity. The responses obtained are shown in Figure 10. For the homopolymer, a typical bistable ferroelectric switching behavior with a hysteresis loop can be seen. In the case of the copolymers, however, the behavior is quite different and the light intensity changes continously as a function of voltage with a slight hysteresis. In order to investigate this effect further, the changes taking place during the application of the voltage were also measured. The optically measured tilt angles at room temperature as a function of voltage for the polymers are shown in Figure 11. For the homopolymer the tilt angle reaches a value of 20° at 10 V. Increasing the voltage further causes only a slight increase in the tilt angle. The temperature dependence of the tilt angle is also shown in Figure 12. It decreases with increasing temperature gradually up to 45 °C, at which the transition to the smectic A phase takes place. In this phase the polymer

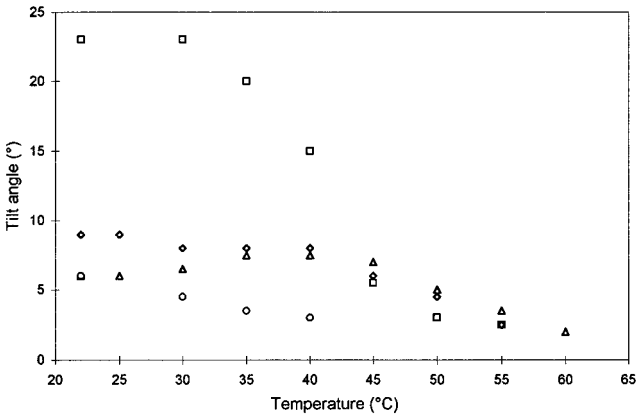

Figure 12. Tilt angle as a function of temperature of homopolymer **I** at 23 V (□) and block copolymers **IV** at 50 V (△), **V** at 60 V (○) and **VI** at 50 V (◇).

shows the electroclinic effect, where the tilt angle is dependent on the applied voltage.

As opposed to the behavior shown by the homopolymer, the block copolymers show much lower optical tilt angles which are also at room temperature highly dependent on the applied voltage. This behavior resembles what is expected of an electroclinic system. However from the X-ray data it is known that the system is in the tilted chiral smectic phase. Furthermore, the X-ray pictures indicate that the molecules are in a tilted arrangement, and in some of the polymers, this tilted arrangement might rotate about a helix. From these X-ray data and from the switching behavior, it could be also conclude that the system can be antiferroelectric or ferrielectric. We assume that the block copolymer is ferroelectric, due to the fact that the homopolymer shows a ferroelectric response. However, the optical tilt angle is much smaller than the angle measured using X-rays. We try to explain this in the following way: during the application of an electric field, not all the molecules become tilted in the same direction with respect to the smectic layers, within the blocks. A domain structure is created along the path of the light where the molecules are oriented in various directions. When observed along this path, molecules might be making various angles with respect to each other, resulting in an avarage tilt angle which is smaller than the cone angle in the smectic phase.

Furthermore, the fact that the intensity transmission curves showed almost no hysteresis indicates that the system is monostable. This is an interesting property which might make such copolymers suitable for display applications in combination with active matrix addressing.

Conclusions

A new family of ferroelectric liquid crystalline block copolymers and the corresponding liquid crystalline homopolymer have been synthesized and characterized. The homopolymer shows a typical ferroelectric behavior at room temperature. The block copolymers had a very narrow molecular weight distribution. Using X-ray diffraction it was established that the blocks were separated. The separation of the blocks was clearly observed in the LC phase of one of the blocks. Both the homopolymer and the copolymers formed chiral tilted smectic phases at room temperature. The homopolymer showed ferroelectric switching with a characteristic hysteresis. The copolymers showed monostable switching which resembled the behavior shown by short pitch FLC where the helix is deformed. The copolymers also showed lower birefringence than the homopolymer, indicating that with the use of such a structure containing isotropic blocks the birefringence of the system can be decreased. This property of the block copolymers, in combination with their monostable switching characteristics, makes them interesting candidates to be used in active matrix addressed displays. However, more work is still needed to increase the optical tilt angle and reduce the switching voltages.

Acknowledgment. A.O. thanks the European Community for a fellowship from the Human Capital and Mobility Programme.

References and Notes

(1) Clark, N. A., Lagerwall, S. T. *Appl. Phys. Lett.* **1980**, *36*, 899.
(2) Shibaev, V. P., Kozlovsky, M. V.; Beresnev, L. A.; Blinov, L. M.; Platé, N. A. *Polym. Bull.* **1984**, *12*, 299.
(3) Uchida, S.; Morita, K.; Miyoshi, K.; Hashimoto, K.; Kawasaki, K. *Mol. Cryst. Liq. Cryst.* **1988**, *155*, 93.
(4) Scherowsky, G.; Schliwa,A.; Springer,J.; Kühnpast,K.; Trapp,W. *Liq. Cryst.* **1989**, *5*, 1281.
(5) Walba, D. M.; Keller, P.; Parmar, D. S.; Clark, N. A.; Wand, M. D. *J. Am. Chem. Soc.* **1989**, *111*, 8273.
(6) Kapitza, H.; Zentel, R.; Twieg, R. J.; Nguyen, C.; Vallerien, S. U.; Kremer, F.; Willson, C. G. *Adv. Mater.* **1990**, *2*, 539.
(7) Dumon, M.; Nguyen, H. T.; Mauzac, M.; Destrade, C.; Achard, M. F.; Gasparoux, H. *Macromolecules* **1990**, *23*, 357.
(8) Shibaev, V. P.; Kozlovsky, M. V.; Platé, N. A.;Beresnev, L. A.; Blinov, L. M. *Liq. Cryst.* **1990**, *8*, 545.
(9) Skarp, K.; Andersson, G.; Lagerwall, S. T.; Kapitza, H.; Poths, H.; Zentel, R. *Ferroelectrics* **1991**, *122*, 127.
(10) Hachiya, S.; Tomoike, K.; Yuasa, K.; Togawa, S.; Sekiya, T.; Takahashi, K.; Kawasaki, K. *J. SID* **1993**, *1/3*, 295.
(11) Svensson, M.; Helgee, B.; Hjertberg, T.; Hermann, D.; Skarp, K. *Polym. Bull.* **1993**, *31*, 167.
(12) Kitzerow, H. S.; Molsen, H.; Heppke, G. *Adv. Mater.* **1992**, *3*, 231.
(13) Hikmet, R. A. M.; Michielsen, M. *Adv. Mater.* **1995**, *7*, 300.
(14) Owen, H.; Coles, H. J.; Newton, J.; Hodge, P. *Mol. Cryst. Liq. Cryst.* **1994**, *257*, 151.
(15) Wischerhoff, E.; Zentel, R. *Liq. Cryst.* **1995**, *18*, 745.
(16) Poths, H.; Wischerhoff, E.; Zentel, R.; Schönfeld, A.; Henn, G.; Kremer, F. *Liq. Cryst.* **1995**, *18*, 811.
(17) Cooray, N.; Kakimoto, M.; Imai, Y.; Suzuki, Y. *Macromolecules* **1995**, *28*, 310.
(18) Dumon, M.; Nguyen, H. T.; Mauzac, M.; Destrade, C.; Gasparoux, H. *Liq. Cryst.* **1991**, *10*, 475.
(19) Naciri, J.; Pfeiffer, S.; Shashidar, R. *Liq. Cryst.* **1991**, *10*, 585.
(20) Naciri, J.; Méry, S.; Pfeiffer, S.; Shashidar, R. *J. SID* **1994**, *2/4*, 175.
(21) Kocot, A.; Wrzalik, R.; Vij, J. K.; Brehmer, M.; Zentel, R. *Phys.Rev. B* **1994**, *50*, 16346.
(22) Helgee, B.; Hjertberg, T.; Skarp, K.; Andersson, G.; Gouda, F. *Liq. Cryst.* **1995**, *18*, 871.
(23) Chiellini, E.; Galli, G.; Lagerwall, S. T.; Komitov, L. *Macromol. Symp.* **1995**, *96*, 79.
(24) Fischer, H.; Poser, S.; Arnold, M.; Frank, W. *Macromolecules* **1994**, *27*, 7133.
(25) Adams, J.; Sanger, J.; Tefehne, C.; Gronski, W. *Macromol. Rapid Commun.* **1994**, *15*, 879.
(26) Bohnert, R.; Finkelmann, H. Macromol. *Chem. Phys.* **1994**, *195*, 689.
(27) Yamada, M.; Iguchi, T.; Hirao, A.; Nakahama, S.; Watanabe, J. *Macromolecules* **1995**, *28*, 50.
(28) Fischer, H.; Poser, S.; Arnold, M. *Macromolecules* **1995**, *28*, 6957.
(29) McKeon, J. E.; Fitton, P. *Tetrahedron* **1972**, *28*, 223.
(30) Percec, V.; Lee, M. *Macromolecules* **1991**, *24*, 1017.
(31) Kamigaito, M.; Meda, Y.; Sawamoto, M.; Higashimura, T. *Macromolecules* **1993**, *26*, 1643.
(32) Ohmura, T.; Sawamoto, M.; Higashimura, T. *Macromolecules* **1994**, *27*, 3714.
(33) Kostromin, S. G.; Sinitsyn, V. V.; Talroze, R. V.; Shibaev, V. P.; Platé, N. A. *Makromol. Chem. Rapid Commun.* **1982**, *3*, 809.
(34) Azároff, L. V. *Mol. Cryst. Liq. Cryst.* **1987**, *145*, 31.
(35) Adams, J.; Gronski, W. *ACS Symp. Ser.* **1990**, *435*, 174.
(36) Fischer, H.; Poser, S.; Arnold, M. *Liq. Cryst.* **1995**, *18*, 503.

MA960185N